THE JOURNAL OF PHYSICAL CHEMISTRY Letters

LETTER

pubs.acs.org/JPCL

Size-Controlled Electron Transfer and Photocatalytic Activity of ZnO−Au Nanoparticle Composites

Jaeil Lee,[†] Hyeong Seop Shim,[‡] Myeongsoon Lee,[†] Jae Kyu Song,*[,‡] and Dongil Lee*[,†]

[†]Department of Chemistry, Yonsei University, Seoul 120-749, Korea

[‡]Department of Chemistry, Kyung Hee University, Seoul 130-701, Korea

Supporting Information

ABSTRACT: This Letter describes size-controlled photocatalytic activity of ZnO nanoparticles coated with glutathione-protected gold nanoparticles with diameters of 1.1, 1.6, and 2.8 nm. The photocatalytic activity of the ZnO−Au composites was found to increase with increasing gold size for both oxidative and reductive catalytic reactions. Photoluminescence decay dynamics of the composites showed that the electron-transfer rate from the photoexcited ZnO to gold nanoparticle also increased as the gold size increased. These results demonstrate that the photogenerated electron transfer and the resulting catalytic activity of the composites can be controlled by the size of the mediating gold capacitors.

SECTION: Nanoparticles and Nanostructures

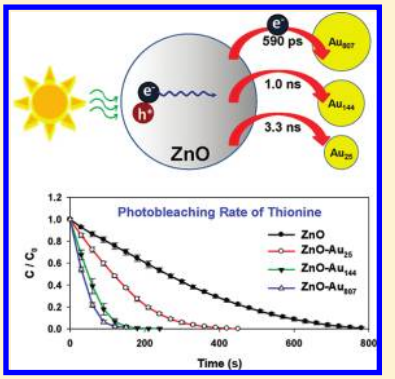

A significant challenge in the research of solar energy conversion and photocatalysts is the rational design of materials that can efficiently trap solar energy, convert into charges, and allow controlled transfer of those charges. Notable breakthroughs have been realized recently in the development of molecular catalysts capable of controlled photogenerated electron transfer.[1−3] However, much less progress has been made in nanoparticle catalysts that often exhibit unique size-dependent physical and chemical properties.[4−7] Combining metal nanoparticles exhibiting quantized charging[8] properties with a light-harvesting unit may lead to nanoparticle composites capable of controlled electron transfer and thereby tunable catalysis. We report here the first quantitative results demonstrating that electron transfer and photocatalytic activity can be controlled by the size of metal nanoparticle in metal−semiconductor composites.

Thiolate-protected gold nanoparticles (AuNPs) with diameters < 3 nm are stable, structurally well-characterized nanoparticles that exhibit size-dependent electrochemical and optical properties.[8−10] One of the most interesting properties of these quantum-sized AuNPs is the ability to control the transfer of electrons into and out of the metallic core. The controllability of the electronic charging is a fundamental result of the ultrasmall capacitance (on the order of aF) of AuNPs. The size-dependent capacitance (C_{AuNP}) has been successfully modeled[8] as a capacitance of metallic spheres with insulating dielectric layers

$$C_{AuNP} = 4\pi\varepsilon_0\varepsilon(r/d)(r + d) \quad (1)$$

where ε_0 is the permittivity of free space, ε, the static dielectric constant of the layer around the metal core, r, the radius of metal core, and d, the layer thickness. The energetics and dynamics of the quantized electronic charging of the AuNPs have been described.[8] In a previous report,[11] we demonstrated that AuNPs acts as an efficient quencher of photoexcited TiO_2 nanoparticles in the colloidal mixture of TiO_2 and AuNPs by accepting electrons from the conduction band of TiO_2 and the quenching process is controlled by the capacitance of AuNP.

In the interest of utilizing this controllability in photocatalysis, we have explored the possibility of controlling the reactivity of ZnO photocatalyst by modifying the surface of ZnO with quantized gold capacitors. Glutathione (GS)-protected AuNPs were synthesized using a modified Brust synthesis[12−14] and solvent-fractionated to obtain size-purified AuNPs (see Supporting Information (SI) for experimental details). The isolated particle sizes determined by transmission electron microscopy (TEM) were 1.1 ± 0.2, 1.6 ± 0.2, and 2.8 ± 0.3 nm (Figure S1, SI), which correspond to AuNP compositions of $Au_{25}(GS)_{18}$, $Au_{144}(GS)_{60}$, and $Au_{807}(GS)_{163}$, respectively.[9,15] Figure 1a shows distinct absorption spectra of these AuNPs; whereas a surface plasmon band at ∼520 nm is observed from Au_{807}, it becomes featureless for Au_{144}, and a steplike absorption profile emerges for Au_{25} due to their discrete energy levels.[9]

Among the linkers that can bind AuNP to ZnO,[16,17] carboxylic groups are known to readily bind to the ZnO surface. Accordingly, GS-protected AuNPs bearing carboxylic acid groups and ZnO

Received: October 2, 2011
Accepted: October 24, 2011
Published: October 24, 2011

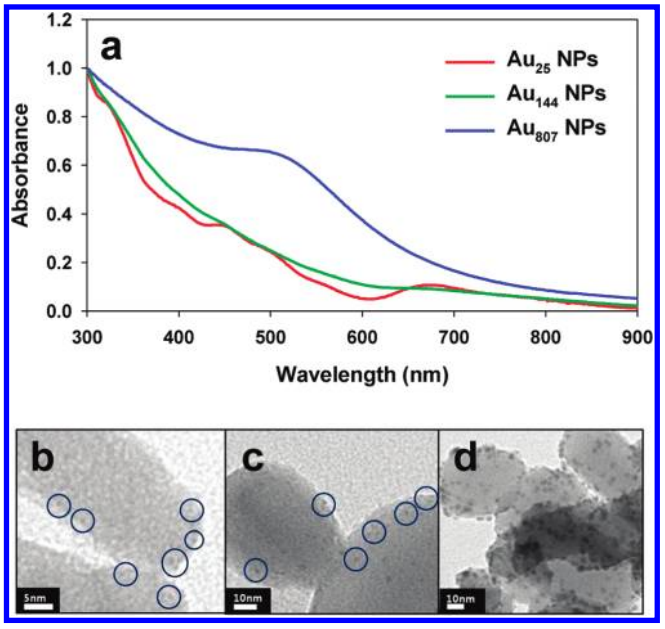

Figure 1. (a) UV−vis absorption spectra of AuNPs and TEM images of (b) ZnO−Au_{25}, (c) ZnO−Au_{144}, and (d) ZnO−Au_{807} composites. In the TEM images, AuNPs are darker than ZnO particles due to their higher electron scattering cross section. Blue circles show the sites where AuNPs are anchored.

nanoparticles were stirred together for 12 h to produce ZnO−Au composites. In this reaction, all AuNPs in the reaction solution were found to completely bind to ZnO, which allowed precise control of AuNP loading by varying the initial concentration of AuNPs in the reaction mixture. This offers special advantage over conventional metal−semiconductor composites[18] in that the size effect of AuNPs can be compared at the same particle loading. Figure 1 shows the TEM images of ZnO−Au composites prepared by reacting 14.4 nmol of Au_{25}, Au_{144}, and Au_{807} NPs with 100 mg of ZnO.[19] Importantly, the sizes of AuNPs on ZnO were all preserved after the anchoring process, emphasizing the advantage of this preparative method.

The photocatalytic activity of ZnO−Au composites was first evaluated by comparing catalytic degradation of a model dye, thionine (TH), by the photoexcited composites. In order to examine the reductive power of the composites alone, photolysis experiments were conducted in a deaerated 1:1 (v/v) CH_3OH-H_2O medium, where CH_3OH acts as an efficient hole scavenger.[20] Photoexcitation of composite colloids (25 mg/L) was conducted using a 150 W xenon lamp with wavelength $\lambda > 320$ nm using a UV cutoff filter (UV-32, HOYA). Photodegradation of the model dye was monitored by recording absorption spectra of the reaction mixtures in situ with a USB 4000 fiber optic spectrometer (Ocean Optics). The absorbance values were averaged out of three independent measurements.

Band gap illumination of ZnO generates electrons in the conduction band, while holes in the valence band are scavenged by CH_3OH. When ZnO is modified with a noble metal, the metal acts as a sink for photogenerated electrons, promoting charge carrier separation.[21] We previously demonstrated that electrons in the photoexcited TiO_2 or ZnO can readily transfer to AuNP protected with thiolate.[20,22] Mulvaney and co-workers also demonstrated that when ZnO is coated with metals such as Au or Ag, electron transfer from photoexcited ZnO to metal occurs and the Fermi levels of the two components equilibrate.[21] The stored electrons on the metal can then participate in the catalytic reaction upon request by the solvent redox species. The photoexcitation and ensuing electron transfer and photocatalytic reduction of TH at a ZnO−Au composite are illustrated in Scheme 1.

The photobleaching rates of TH by ZnO, ZnO−Au_{25}, ZnO−Au_{144} and ZnO−Au_{807} are compared in Figure 2a. All composite suspensions were irradiated equally, and the change in absorbance at 600 nm was recorded during photocatalytic reaction (Figure S2, SI). Note that the catalytic activity increased with increasing AuNP loading, as shown in Figure S3 (SI) for 1, 2, and 3 wt % Au_{807} loaded composites. Because of this loading effect, we compared the catalytic activity at the same particle concentration. As shown in Figure S4A (SI), there was some photobleaching of TH observed (∼12% at 300 s) in the absence of catalysts, but the rate of the photobleaching drastically increased in the presence of all catalysts, as can be seen in Figure 2a. The bleaching rates are, however, vastly different depending on the catalyst used. The photolysis time ($t_{1/2}$) corresponding to 50% degradation of TH was 260 s with ZnO. The rate became dramatically faster with the modification of AuNPs; $t_{1/2}$ values decreased to 112, 47, and 34 s with ZnO−Au_{25}, ZnO−Au_{144}, and ZnO−Au_{807} composites, respectively. The dramatic increase in the catalytic activity with increasing AuNP size indicates that large AuNP extracts electrons more efficiently than small AuNP, and as a result, more electrons are separated in the composite as the AuNP size increases. We also note that the size effect observed here is not merely due to the difference in surface area. Photolysis of TH with 3 wt % of Au_{25}, Au_{144}, and Au_{807} (i.e., different particle concentrations) shown in Figure S5 (SI) shows that the activity is again the highest with Au_{807}, even though the total surface areas of AuNPs are ∼3- and 2-fold larger, respectively, with Au_{25} and Au_{144} than that with Au_{807}.

The enhanced charge separation in the presence of AuNPs on ZnO also implies that more photogenerated holes become available in the composite. Thus, we examined the oxidative catalytic activity of the composites with rhodamine 6G (R6G), which is known to undergo oxidative degradation in water.[22,23] Accordingly, photolysis experiments were carried out with composites (50 mg/L) in water under atmospheric conditions. Figure 2b compares the photobleaching rates of R6G by ZnO, ZnO−Au_{25}, ZnO−Au_{144}, and ZnO−Au_{807}. The photobleaching of R6G was negligible in the absence of catalyst, as shown in Figure S4B (SI), but it significantly increased in the presence of catalysts. Overall, the photobleaching of R6G occurs at a longer time scale than that of TH, but the AuNP size effect can be clearly observed. The $t_{1/2}$ of R6G was 8.9 min with ZnO, which gradually decreased with increasing AuNP size; $t_{1/2}$ were 5.4, 4.0, and 3.0 min with ZnO−Au_{25}, ZnO−Au_{144}, and ZnO−Au_{807}, respectively. Again, the evident size effect can be ascribed to the increased charge separation with increasing AuNP size. The above catalytic results undoubtedly reveal that the AuNP as an electron acceptor plays a key role in the enhanced photocatalysis. The electron-receiving power of AuNP increases with increasing size, which can be understood by the size-dependent capacitance model.[8,11]

If indeed the charge separation is affected by the size of AuNPs, it may be possible to monitor the AuNP size effect on the dynamics of photogenerated electrons. Photoluminescence (PL) of ZnO has been utilized as a probe to investigate the charge distribution and Fermi level equilibration in metal and semiconductor

Scheme 1. Photoexcitation, Electron Transfer, and Photocatalytic Reduction of TH at a ZnO−Au Composite

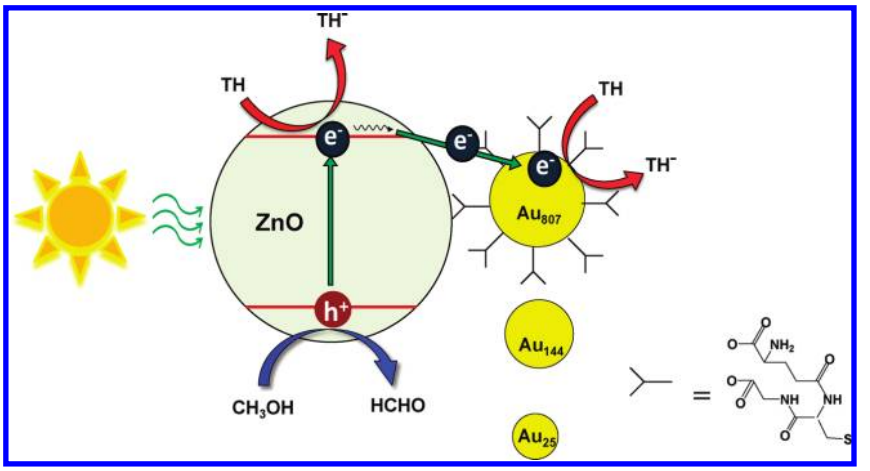

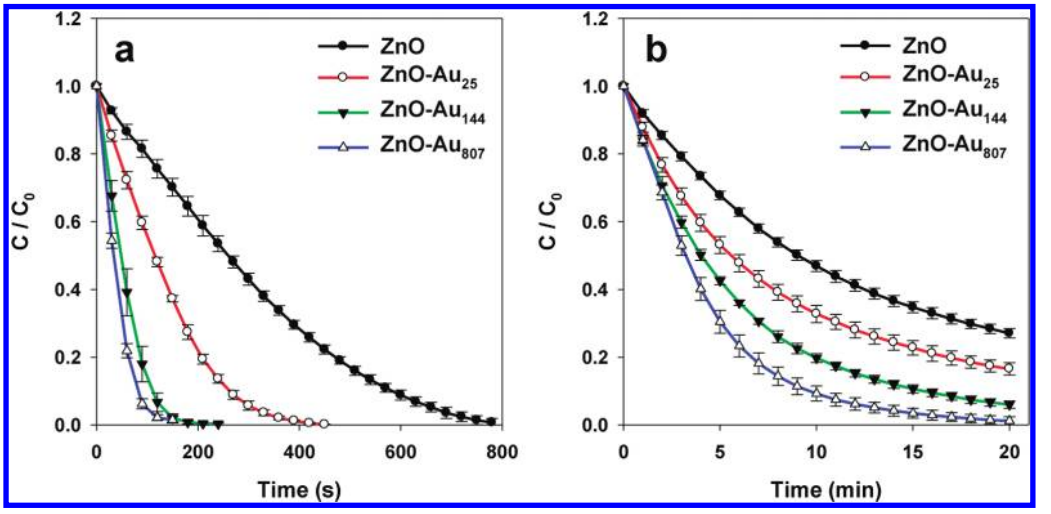

Figure 2. Change in (a) TH and (b) R6G concentration (C) relative to the initial concentration (C_0) during photocatalysis with ZnO and ZnO−Au composites. The concentrations of TH (C_0 = 25 μM) and R6G (C_0 = 12.5 μM) were estimated from the absorbance values at 600 and 525 nm, respectively. The absorption spectra recoded during the photolysis reactions of TH and R6G are shown in Figures S2 and S6 (SI), respectively.

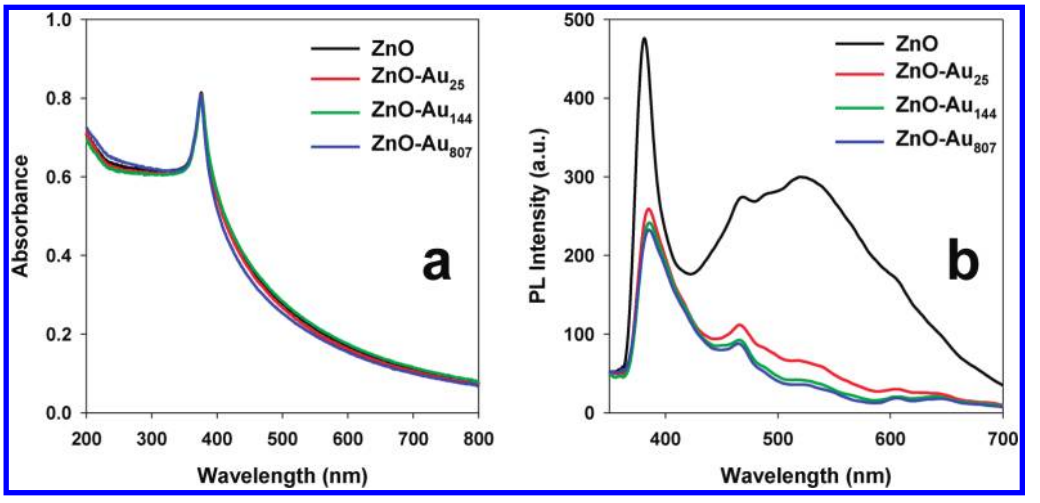

Figure 3. (a) Optical absorption spectra and (b) PL spectra (λ_{EX} = 290 nm) of ZnO and ZnO−Au composites in 1:1 CH_3OH−H_2O solution.

dx.doi.org/10.1021/jz2013352 |J. Phys. Chem. Lett. 2011, 2, 2840–2845

composites.[24] The absorption and PL spectra of ZnO and composites are shown in Figure 3a and b, respectively. Whereas the absorbance spectra show little change upon the modification with AuNP, both band edge emission at 380 nm and broad emission at around 520 nm that is related with the charge carrier relaxation via surface-related trap states[25] are found to be drastically quenched in the presence of AuNPs, suggesting their strong influence on the carrier dynamics.

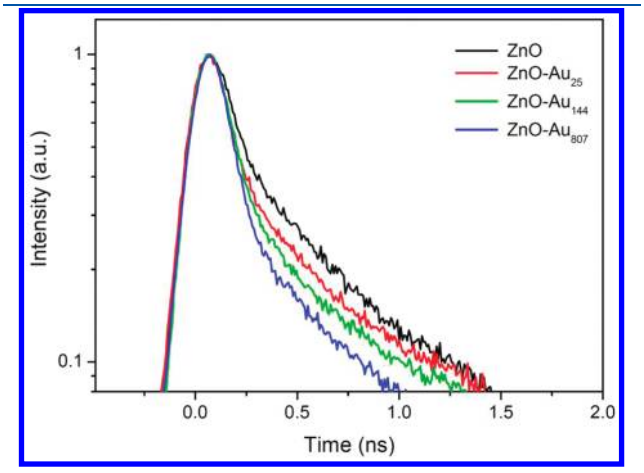

Figure 4. Decay profiles of the exciton emission of ZnO and ZnO−Au composites in deaerated a 1:1 CH_3OH-H_2O medium obtained using the time-correlated single-photon counter technique. Intensities are normalized for comparison purposes.

To further probe the electron-transfer process in ZnO−Au composites, we carried out a time-resolved PL study of ZnO and the composites. The band edge emission of ZnO decays by the electron−hole recombination in deaerated a 1:1 CH_3OH-H_2O medium, as shown in Figure 4. The decay profile is fitted most reasonably by a biexponential model (see SI for details).[26] The fitting shows that the fast component, τ_1 (0.15 ns), that is thought to arise from the free exciton states[27,28] is the major deactivation pathway (80%) and became shorter in the presence of AuNPs. The exciton lifetimes of the composites were found to be 0.14, 0.13, and 0.12 ns for ZnO−Au_{25}, ZnO−Au_{144}, and ZnO−Au_{807}, respectively. This result suggests that electron transfer from ZnO to AuNP forms an additional deactivation pathway, and the electron-transfer efficiency increases with increasing AuNP size. Assuming that the difference in the exciton lifetimes is only due to the added electron-transfer process,[26] the electron-transfer rate constants (k_{ET}) in ZnO−Au composites are estimated to be 0.3×10^9, 1.0×10^9, and 1.7×10^9 s^{-1} for ZnO−Au_{25}, ZnO−Au_{144}, and ZnO−Au_{807}, respectively, using τ_1 of ZnO and the composites

$$k_{ET} = 1/\tau_1(ZnO-Au) - 1/\tau_1(ZnO) \quad (2)$$

The electron-transfer efficiencies from ZnO to AuNPs can then be calculated to be 5, 13, and 20% for ZnO−Au_{25}, ZnO−Au_{144}, and ZnO−Au_{807}, respectively. The decay profiles of ZnO and the composites in water medium are found to be similar, as shown in Figure S7 (SI), except for slightly shorter time constants in the water medium. These PL results unambiguously confirm that electron transfer occurs from photoexcited ZnO to AuNP, and the electron-transfer efficiency increases with AuNP size. The enhanced

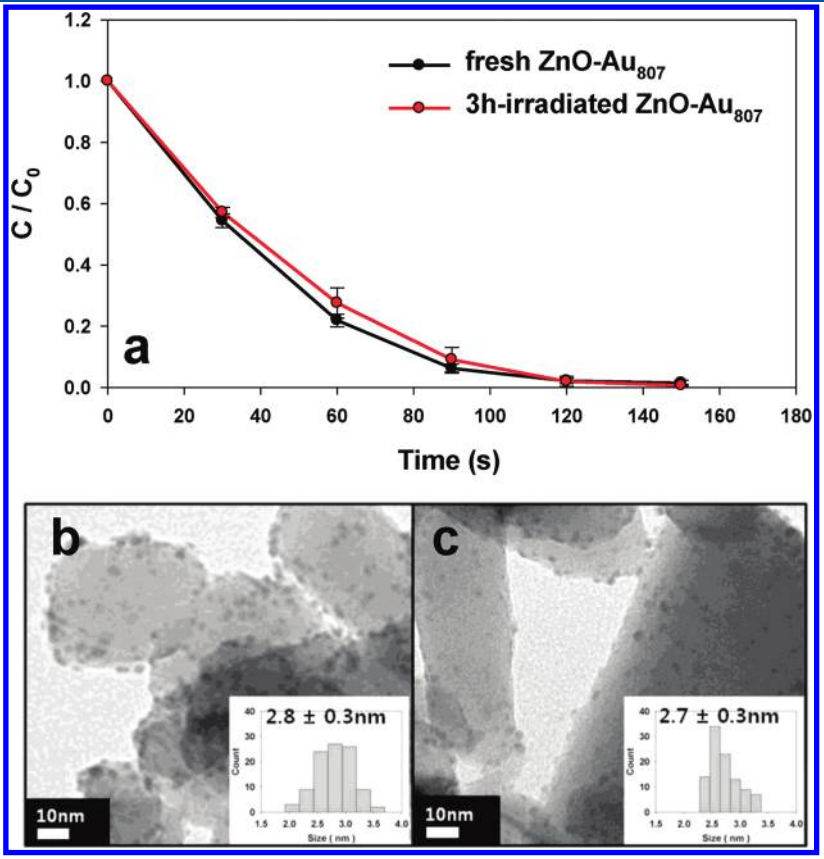

Figure 5. (a) Comparison of the photobleaching rate of TH with fa reshly prepared ZnO−Au_{807} composite (black line) and the same composite after photoirradiation for 3 h in deaerated 1:1 CH_3OH-H_2O (red line). TEM images of the ZnO−Au_{807} composite (b) before and (c) after 3 h of irradiation.

dx.doi.org/10.1021/jz2013352 |J. Phys. Chem. Lett. 2011, 2, 2840–2845

photocatalytic activity observed in Figure 2a and b can thus be understood by the enhanced charge separation in the composite, which can be controlled by the size of AuNPs.

Finally, the photostability of composite catalysts was examined by comparing the photocatalytic activity of the composites before and after photoirradiation. As can be seen in Figure 5a, the photobleaching rates of TH are almost identical with freshly prepared ZnO−Au_{807} composites and 3-h-irradiated ZnO−Au_{807} composites. TEM images shown in Figure 5b and c also show that the average particle size and distribution of AuNPs on ZnO are preserved after 3 h of irradiation. These results show that GS ligands and the carboxylate binding groups on ZnO are reasonably stable against UV−vis irradiation ($\lambda > 320$ nm).

In summary, these are the first results demonstrating that electron transfer from photoexcited ZnO to AuNPs and the resulting photocatalytic activity can be controlled by the size of the mediating gold capacitor. These results may open the avenue to utilize the unique charging properties of quantum-sized AuNPs in the development of photocatalysts capable of selective reactions via the control of electron flow.

■ ASSOCIATED CONTENT

Supporting Information. Experimental details including syntheses of AuNPs, photocatalysis, and time-resolved PL experiments and supplementary TEM images and photocatalysis results. This material is available free of charge via the Internet at http://pubs.acs.org.

■ AUTHOR INFORMATION

Corresponding Author

*E-mail: dongil@yonsei.ac.kr (D.L.); jaeksong@khu.ac.kr (J.K.S.).

■ ACKNOWLEDGMENT

This research was supported by the Mid-Career Researcher Program (2011-0029735), Basic Science Research Program (2010-0009244 and 2009-0068705), World Class University Program (R32-2008-000-10217-0), and Priority Research Centers Program (2009-0093823) through an NRF grant funded by the Ministry of Education, Science and Technology, and Yonsei University Research Fund.

■ REFERENCES

(1) Dempsey, J. L.; Esswein, A. J.; Manke, D. R.; Rosenthal, J.; Soper, J. D.; Nocera, D. G. Molecular Chemistry of Consequence to Renewable Energy. *Inorg. Chem.* **2005**, *44*, 6879–6892.

(2) Heyduk, A. F.; Nocera, D. G. Hydrogen Produced from Hydrohalic Acid Solutions by a Two-Electron Mixed-Valence Photocatalyst. *Science* **2001**, *293*, 1639–1641.

(3) Fukuzumi, S.; Okamoto, K.; Tokuda, Y.; Gros, C. P.; Guilard, R. Dehydrogenation versus Oxygenation in Two-Electron and Four-Electron Reduction of Dioxygen by 9-Alkyl-10-methyl-9,10-dihydroacridines Catalyzed by Monomeric Cobalt Porphyrins and Cofacial Dicobalt Porphyrins in the Presence of Perchloric Acid. *J. Am. Chem. Soc.* **2004**, *126*, 17059–17066.

(4) Subramanian, V.; Wolf, E. E.; Kamat, P. V. Catalysis with TiO_2/Gold Nanocomposites. Effect of Metal Particle Size on the Fermi Level Equilibration. *J. Am. Chem. Soc.* **2004**, *126*, 4943–4950.

(5) Robel, I.; Kuno, M.; Kamat, P. V. Size-Dependent Electron Injection from Excited CdSe Quantum Dots into TiO_2 Nanoparticles. *J. Am. Chem. Soc.* **2007**, *129*, 4136–4137.

(6) Jakob, M.; Levanon, H.; Kamat, P. V. Charge Distribution between UV-Irradiated TiO_2 and Gold Nanoparticles: Determination of Shift in the Fermi Level. *Nano Lett.* **2003**, *3*, 353–358.

(7) Cozzoli, P. D.; Fanizza, E.; Comparelli, R.; Curri, M. L.; Agostiano, A.; Laub, D. Role of Metal Nanoparticles in TiO_2/Ag Nanocomposite-Based Microheterogeneous Photocatalysis. *J. Phys. Chem. B* **2004**, *108*, 9623–9630.

(8) Murray, R. W. Nanoelectrochemistry: Metal Nanoparticles, Nanoelectrodes, and Nanopores. *Chem. Rev.* **2008**, *108*, 2688–2720.

(9) Jin, R. Quantum Sized, Thiolate-Protected Gold Nanoclusters. *Nanoscale* **2010**, *2*, 343–362.

(10) Varnavski, O.; Ramakrishna, G.; Kim, J.; Lee, D.; Goodson, T. Critical Size for the Observation of Quantum Confinement in Optically Excited Gold Clusters. *J. Am. Chem. Soc.* **2010**, *132*, 16–17.

(11) Kim, J.; Lee, D. Size-Controlled Interparticle Charge Transfer between TiO_2 and Quantized Capacitors. *J. Am. Chem. Soc.* **2007**, *129*, 7706–7707.

(12) Schaaff, T. G.; Whetten, R. L. Giant Gold−Glutathione Cluster Compounds: Intense Optical Activity in Metal-Based Transitions. *J. Phys. Chem. B* **2000**, *104*, 2630–2641.

(13) Negishi, Y.; Nobusada, K.; Tsukuda, T. Glutathione-Protected Gold Clusters Revisited: Bridging the Gap between Gold(I)−Thiolate Complexes and Thiolate-Protected Gold Nanocrystals. *J. Am. Chem. Soc.* **2005**, *127*, 5261–5270.

(14) Wu, Z.; Chen, J.; Jin, R. One-Pot Synthesis of $Au_{25}(SG)_{18}$ 2- and 4-nm Gold Nanoparticles and Comparison of Their Size-Dependent Properties. *Adv. Funct. Mater.* **2011**, *21*, 177–183.

(15) Hostetler, M. J.; Wingate, J. E.; Zhong, C.-J.; Harris, J. E.; Vachet, R. W.; Clark, M. R.; Londono, J. D.; Green, S. J.; Stokes, J. J.; Wignall, G. D.; Glish, G. L.; Porter, M. D.; Evans, N. D.; Murray, R. W. Alkanethiolate Gold Cluster Molecules with Core Diameters from 1.5 to 5.2 nm: Core and Monolayer Properties as a Function of Core Size. *Langmuir* **1998**, *14*, 17–30.

(16) Im, J.; Singh, J.; Soares, J. W.; Steeves, D. M.; Whitten, J. E. Synthesis and Optical Properties of Dithiol-Linked ZnO/Gold Nanoparticle Composites. *J. Phys. Chem. C* **2011**, *115*, 10518–10523.

(17) Keis, K.; Lindgren, J.; Lindquist, S.-E.; Hagfeldt, A. Studies of the Adsorption Process of Ru Complexes in Nanoporous ZnO Electrodes. *Langmuir* **2000**, *16*, 4688–4694.

(18) Kamat, P. V. Photophysical, Photochemical and Photocatalytic Aspects of Metal Nanoparticles. *J. Phys. Chem. B* **2002**, *106*, 7729–7744.

(19) These reactions resulted in composites with 0.15 wt% Au_{25}, 0.67 wt% Au_{144}, and 3 wt% Au_{807} NP to ZnO, respectively.

(20) Lee, M.; Amaratunga, P.; Kim, J.; Lee, D. TiO_2 Nanoparticle Photocatalysts Modified with Monolayer-Protected Gold Clusters. *J. Phys. Chem. C* **2010**, *114*, 18366–18371.

(21) Wood, A.; Giersig, M.; Mulvaney, P. Fermi Level Equilibration in Quantum Dot−Metal Nanojunctions. *J. Phys. Chem. B* **2001**, *105*, 8810–8815.

(22) Udawatte, N. Gold Nanoparticle-Modified Zinc Oxide Nanoparticles As Novel Photocatalytic Materials. Ph.D. Thesis, Western Michigan University, 2010.

(23) Amaratunga, P.; Lee, M.; Kim, J.; Lee, D. Preparation and Photocatalytic Activity of TiO_2 Nanocomposites Coated with Monolayer-Protected Gold Clusters. *Can. J. Chem.* **2011**, *89*, 1001–1009.

(24) Subramanian, V.; Wolf, E. E.; Kamat, P. V. Green Emission to Probe Photoinduced Charging Events in ZnO−Au Nanoparticles. Charge Distribution and Fermi-Level Equilibration. *J. Phys. Chem. B* **2003**, *107*, 7479–7485.

(25) Vanheusden, K.; Warren, W. L.; Seager, C. H.; Tallant, D. R.; Voigt, J. A.; Gnade, B. E. Mechanisms Behind Green Photoluminescence in ZnO Phosphor Powders. *J. Appl. Phys.* **1996**, *79*, 7983–7990.

(26) Tvrdy, K.; Frantsuzov, P. A.; Kamat, P. V. Photoinduced Electron Transfer from Semiconductor Quantum Dots to Metal Oxide Nanoparticles. *Proc. Natl. Acad. Sci. U.S.A.* **2011**, *108*, 29–34.

(27) Jung, S. W.; Park, W. I.; Cheong, H. D.; Yi, G.-C.; Jang, H. M.; Hong, S.; Joo, T. Time-Resolved and Time-Integrated

Photoluminescence in ZnO Epilayers Grown on Al_2O_3(0001) by Metalorganic Vapor Phase Epitaxy. *Appl. Phys. Lett.* **2002**, *80*, 1924–1926.

(28) Bertram, F.; Christen, J.; Dadgar, A.; Krost, A. Complex Excitonic Recombination Kinetics in ZnO: Capture, Relaxation, And Recombination from Steady State. *Appl. Phys. Lett.* **2007**, *90*, 041917/1–041917/3.